Green Chemistry

Accepted Manuscript

ROYAL SOCIETY OF CHEMISTRY

www.rsc.org/greenchem

# Mechanistic Insights into Lignin Depolymerisation in Acidic Ionic Liquids

Gilbert F. De Gregorio[a], Cameron C. Weber[a], John Gräsvik[a], Tom Welton[*,a], Agnieszka Brandt[b] and Jason P. Hallett[*,b]

[a]*Department of Chemistry, Imperial College London, London, SW7 2AZ, United Kingdom;* t.welton@imperial.ac.uk

[b]*Department of Chemical Engineering, Imperial College London, London, SW7 2AZ, United Kingdom;* j.hallett@imperial.ac.uk

Acidic anions of ionic liquids have been demonstrated as efficient catalysts for the cleavage of the β-*O*-4 ether linkage prevalent in the lignin superstructure. Through the use of lignin model compounds with varying functionality and by monitoring reaction kinetics, a full mechanistic investigation into the hydrolysis of the β-*O*-4 linkage in acidic ionic liquid solutions is reported. Hammett acidities are reported for different 1-butyl-3-methylimidazolium hydrogen sulfate $[C_4C_1im][HSO_4]$ ionic liquid systems with varying acid and water concentrations and were correlated to substrate reactivity. Results show that the rate of ether cleavage increases with an increase in acidity and the initial dehydration of the model compound is the rate-determining step of the reaction. The Eyring activation parameters of the reaction in hydrogen sulfate ionic liquids with a variety of cations are reported, indicating a consistent E1 dehydration mechanism. Hydrogen bonding in protic ionic liquids was shown to significantly influence anion-cation interactions, consequently altering the solvation of the protonated starting material and therefore the overall rate of reaction. Comparison of reaction rates in these ionic liquids with results within aqueous or aqueous/organic media indicate that the ionic liquids facilitate more rapid cleavage of the β-*O*-4 ether linkage even under less acidic conditions. All the reported results give a complete overview of both the mechanistic and solvation effects of acidic ionic liquids on lignin model compounds and provide scope for the appropriate selection and design of ionic liquids for lignin processing.

## Introduction

Lignin, a major component of woody biomass, is the second most naturally abundant polymer on earth after cellulose, accounting for up to 30% by weight of lignocellulosic biomass.[1] Biosynthesized from the three main monolignols: sinapyl alcohol, coniferyl alcohol and *p*-coumaryl alcohol, lignin has a complex amorphous polyphenolic structure with a range of different bonding motifs that link the monomers together. The β-*O*-4 ether linkage has been identified to be the most prevalent inter-unit linkage in the macrostructure, responsible for up to 50 % of all bonding and is also known to be the most susceptible to cleavage under acidic conditions.[2,3] This has fuelled many studies in the targeted cleavage of this linkage to isolate and extract a range of aromatic platform chemicals.

The use of ionic liquids (ILs) in biomass processing has received a surge in interest with the focus principally directed at the efficient fractionation of lignocellulosic biomass into its constituent oligomeric and monomeric components.[4] Although many of these IL systems involve imidazolium-based cations, the anion has shown to be of primary importance in many aspects of bio-processing, including the solubility of lignocellulose,[5-7] cellulose dissolution,[8,9] selective lignin dissolution[10-12] and lignin fragmentation and isolation.[13] The high structural versatility of ILs has led to these being commonly coined "designer solvents" due to their ability to act as acids, bases and nucleophiles as well as recyclable solvents with negligible vapour pressures.[14]

Whilst studies have been reported demonstrating successful fractionation of the carbohydrate rich material from lignin[11,15] the modification of the lignin structure during depolymerisation is not well understood with studies focusing on the change in molecular weight and polydispersity.[16,17,18] This has encouraged significant mechanistic investigations into how ethers in lignin cleave in IL media, as fundamental understanding of the role of the reaction medium is paramount for downstream lignin processing. In order to simplify the complexity of the lignin macromolecule, many model compounds containing phenyl-alkyl ethers have been previously tested under a range of conditions. A common model compound studied in the literature, guaiacylglycerol-β-guaiacol ether (which will henceforth be referred to as compound **I**),[19-22] represents one repeating unit bearing the β-*O*-4 ether linkage also incorporating aryl-methoxy and hydroxyl groups.

In two studies, Cox *et al* reported the use of protic ILs, namely $[HC_1im]$ with $Br^-$, $Cl^-$, $[BF_4]^-$ and $[HSO_4]^-$ anions, for the successful cleavage of **I** to guaiacol.[19,20] This process was then applied to oak wood lignin isolated after the cellulose component was precipitated and removed from the biomass dissolved in $[C_2C_1im][OAc]$.[23] A similar study was also reported whereby a range of chlorometallate Lewis acids were included with $[C_4C_1im]Cl$ to hydrolyze the model compound **I** to guaiacol upon addition of water.[21.] Although these investigations show the importance of acidity, no correlation between Hammett acidity and yield was established due to the differences in the nucleophilicities of the anions. Other studies have shown the possibility of such model compounds undergoing an initial dehydration to form enol-ether like intermediates[19,22,24] as the presence of these intermediates has been identified when a range of ILs with non-nucleophilic basic anions were used.

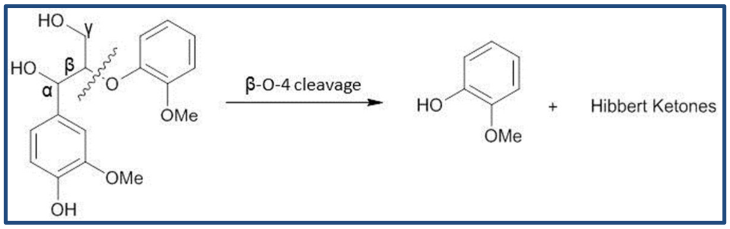

**Fig 1.** Cleavage of β-*O*-4 ether linkage in model compound **I**

Computational investigations have led to similar mechanistic pathways being postulated. Density functional theory has shown that the carbocation formed during the dehydration exhibits the highest energy along the reaction pathway.[24] This accords with the experimental observation that the presence of electron donating groups, such as methoxy or hydroxy substituents commonly found in lignin, promotes the cleavage of the ether linkage.[24] This investigation attempted to identify the key intermediates and transition states of a range of lignin model compounds showing promise toward understanding the mechanism of lignin depolymerisation. However, the use of aqueous sulfuric acid as the reaction medium limits the understanding of the role of water and does not provide insight into the role of IL solvent effects in the process.

Herein, our investigation aims to reconcile former discrepancies in elucidating the mechanism of β-*O*-4 ether cleavage in ILs whereby the roles of acid, water and substrate functionality are all variables that aid in identifying the rate-determining step of the reaction. In order to study a range of substrate functionalities, the model compounds 2-phenoxy-1-phenylethanol (**II**), 2-(2-methoxyphenoxy)-1-phenylethanol (**III**), 1-(3,4-dimethoxyphenyl)-2-(2-methoxyphenoxy)ethanol (**IV**) and *erythro*-1-(3-methoxy-4-*O*-benzylphenyl)-2-(2-methoxyphenoxy)-l,3-propanediol (**V**) (Fig. 2) were all prepared and their relative reactivities analyzed. Through the use of reaction kinetics and linear-free energy relationships, the fundamental interactions of acidic ILs (Fig. 3) with the model compound **I** are assessed. Finally, the reaction's activation parameters were obtained experimentally, giving insight into the mode of solvation of the starting material by the IL.

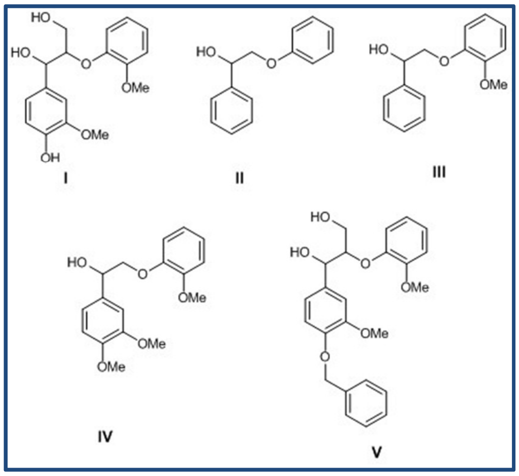

**Fig. 2**: Model compounds bearing β-*O*-4 ether linkages used in this investigation.

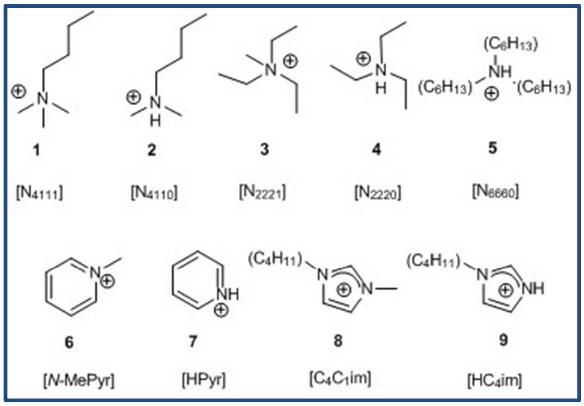

**Fig. 3**: Protic and aprotic $[HSO_4]^-$ IL cations investigated for ether cleavage.

## Experimental

### Procedure for Kinetic studies

Compound **I** was initially dissolved in ethyl acetate and made up to 10 mL using a volumetric flask. Aliquots of this solution containing *circa.* 0.5 mg of compound I were placed in 8 × 2 mL glass vials and the solvent was left to evaporate overnight, leaving the dry substrate. The ILs were vacuum dried overnight at 80 °C before use and 100 mg of the ionic liquid was then added, followed by the required amount of water. The vials were sealed and inserted into a heating module (VWR digital heating block) for the allotted amount of time at the required temperature and subsequently cooled in a dry ice-ethanol mixture. 500 µL of an acetonitrile solution containing the internal standard 3,4,5-trimethoxybenzaldehyde was then added with the vial made up to 1 mL through further addition of deionized water. The contents of the vial were then analyzed by HPLC (further details are provided in the ESI).

### Procedure for reactivity of model compounds

A round bottom flask was charged with 25 mg of the model compound (**I**-**V**) along with a stirring flea, 1 g of the IL and 200 µL of distilled water. The reaction mixture was left to stir for 5 hours at 100 °C under a steady flow of nitrogen gas. The reaction was then quenched with 1 mL of distilled water and the products extracted with chloroform (3 × 1 mL). The organic washings were then combined and the solvent removed under reduced pressure to yield the dry products, which were then analyzed by HSQC spectroscopy.

## Results

In our study, the archetypal model compound **I** was selected to realistically represent the β-*O*-4 linkage in softwood lignin. 1-butyl-3-methylimidazolium hydrogen sulfate ($[C_4C_1im][HSO_4]$) was selected as the primary IL of study as it has been used in the deconstruction of lignocellulosic biomass[11] and its lignin products have been identified.[18] In this process the anion conveniently acts as both a proton source and nucleophile. In order to identify the rate-determining step of the reaction, kinetic data were obtained exploring the effects of both acidity and water through varying the quantity of both in each reaction. The hydrolyzed guaiacol product was determined by HPLC and used as an indicator of the degree of ether cleavage. Calibration of guaiacol response to concentration allowed quantitative measurement of the product concentration *via* HPLC. Rate constants for each IL system were obtained using pseudo-first order reaction conditions with respect to the ether substrate, with the IL in large excess. A representative reaction profile is provided in the ESI. Mixtures of IL with varying acid and water content were prepared as outlined in the experimental procedure. Excess acid quantities studied included 0, 10 and 20 mol % sulfuric acid to the IL (herein labelled as $[C_4C_1im][HSO_4]_{x\%}$ where x denotes the amount of acid added to the IL). Water contents in each system ranged from 0 to 50 (wt/wt) % with respect to the IL reaction medium.

### The effects of water and acid

The reaction of the model compound at 100 °C in [$C_4C_1$im][$HSO_4$] with no added acid provided 4 rate constants between 0 and 23 (wt/wt) % water to IL (Fig 4a) due to the slow reaction progress at higher water concentrations. In ILs with added acid, 9 rate constants from 9.09 to 50 (wt/wt) % water were collected. In the IL system with no added acid, the addition of water appears to have no discernible influence on the rate of reaction within this range. With both the 10 and 20 mol % acid-IL systems, small increases in rate are observed for low concentrations of added water with a significant decrease in rate by over half an order of magnitude observed when reaction media with over 35 (wt/wt) % of water: IL are employed (Fig. 4b and c). This decrease in rate most likely occurs due to the reduction of acidity as a result of the dilution of the medium, consistent with the protonation of compound I occurring prior to the rate determining step, as will be discussed in more detail below.

**4a**

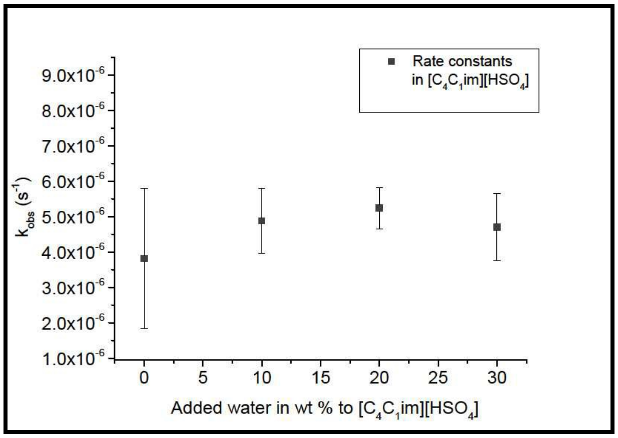

**4b**

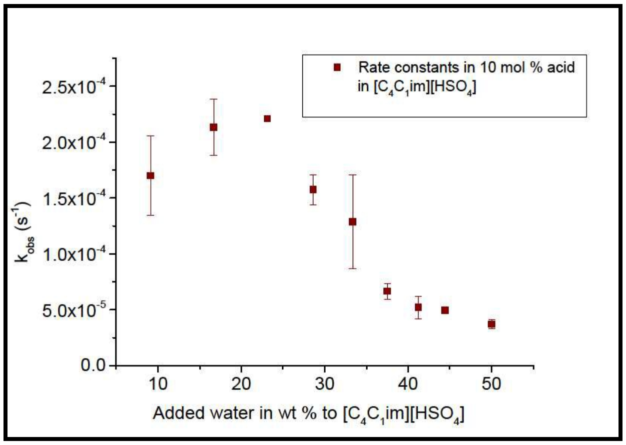

**4c**

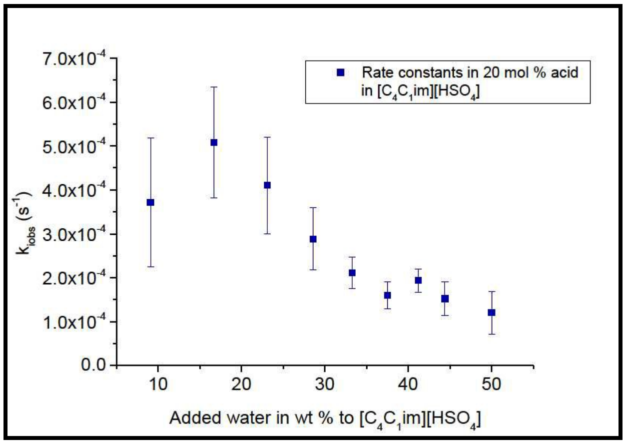

**Fig. 4** Effect of water in [$C_4C_1$im][$HSO_4$] on rate of reaction of the hydrolysis **I** at 100 °C with **a.** no added acid, **b.** 10 mol % acid, **c.** 20 mol % acid. Error bars represent the standard deviation from triplicate measurements,

To scrutinize the effects of water in modifying the acidity of the IL system, the acidity of each IL, acid and water system were measured. Hammett acidity, a method allowing the measurement of acidity in non-aqueous media[25] was used and the Hammett acidity values ($H_0$) are reported in Fig. 5. When water was added to systems with 10 and 20 mol % acid, a relative decrease in acidity was observed with the $H_0$ value reaching a maximum between 20 and 30 (wt/wt) % water: IL compared with systems with less water. However, in systems with higher quantities of water, no decrease in Hammett acidity is observed. Where one would expect dilution of the acidic media from the addition of water to the acidic IL, acidity is actually seen to plateau, showing high quantities of water maintaining the same proton transfer ability within the reaction medium.

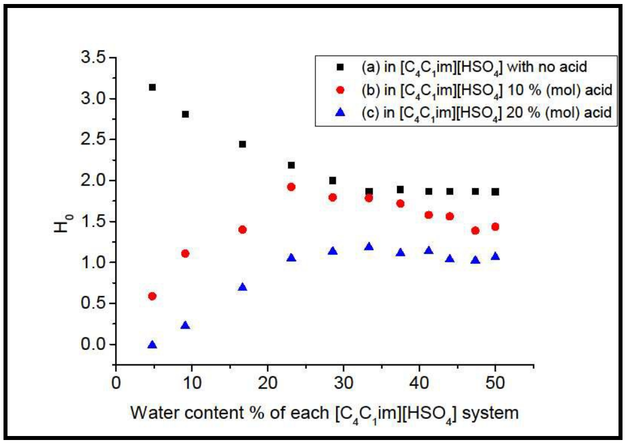

**Fig. 5** $H_0$ values of water: [$C_4C_1$im][$HSO_4$] systems (wt/wt %)
**a.** no added acid (black squares), **b.** 10 mol % acid (red circles) **c.** 20 mol % acid (blue diamonds). Uncertainties are smaller than the size of the data point hence are not included in the figure.

As an increase in water was seen to significantly decrease the reaction rate of the hydrolysis of **I**, this implies a competing effect of water, with its presence impeding reaction progress. This can be further observed when the rate constants are directly correlated to the Hammett acidity of each IL-acid-water system, as shown in Fig 6. If water had the sole effect of increasing acidity as a proton transfer medium or diluting the acid, a direct correlation between Hammett acidity and rate would be observed. It is clear that poorly acidic systems in general exhibit slower rates as shown by the three coloured regions in Fig 6 whereby $[C_4C_1im][HSO_4]_{20\%\ acid}$ displays the highest reaction rates and $[C_4C_1im][HSO_4]_{0\%\ acid}$ the lowest. The lack of trend within each IL-acid medium infers a mechanism in which water affects reactivity beyond its role in proton transport, suggesting water is implicated in the reaction prior to the rate-determining step. Further evidence of the competing effect of water is presented when examining the trend in Fig. 5a, where the addition of water increases acidity, as there is no overall increase in rate due to the increased presence of water in this system, potentially indicating that water is inhibiting a dehydration process. To summarize, the lack of direct correlation between Hammett acidity and rate constant implies water has multiple roles, by influencing acidity but also in impeding substrate reactivity.

Through this investigation, it is clear that the hydrolysis of **I** requires initial protonation of the substrate followed by a dehydration step where the presence of high quantities of water retards reaction progress. This is then followed by the hydrolysis of the intermediate in the presence of water. The small increases in rate with small quantities of added water shown in Figs 4b and 4c support this hypothesis, as the addition of 15-20 % water allowed sufficient hydrolysis to occur whilst limiting the impeding effects of water on dehydration. Similar observations been reported in a computational study by Janesko and with studies on model compound I by Yu *et al*, where the dehydrated intermediate is able to form in dry $[C_4C_1im]Cl$ and undergoes hydrolysis only upon upon the addition of water.[26,27] Comparing this mechanism with others proposed in literature,[19,22,24] the dehydration of **I** appears as the plausible reaction route prior to ether cleavage.

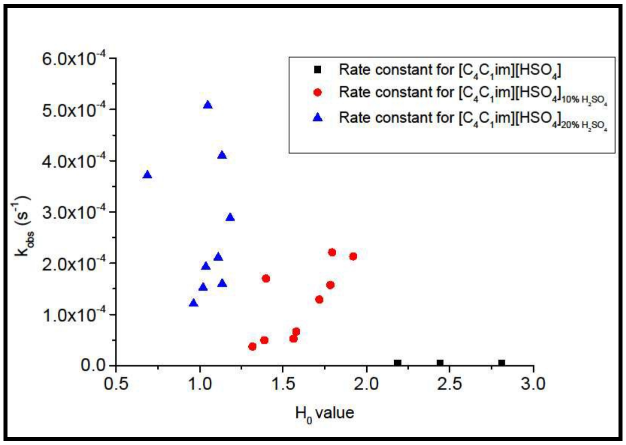

**Fig. 6** Attempted correlation of rate constant with Hammett acidity

## Model compound reactivity: Importance of functionality

To further confirm the importance of dehydration in lignin depolymerisation, an investigation into varying the functionality of the substrate in a highly acidic system was carried out. Five model compounds bearing the β-*O*-4 ether linkage were left to react for 5 hours in $[C_4C_1im][HSO_4]_{10\%\ acid}$, extracted, redissolved in $CDCl_3$ and analyzed *via* 2D-HSQC NMR to determine whether hydrolysis occurred. Compound **I** includes a number of electron-donating groups around both aromatic moieties that can both activate the β-*O*-4 ether linkage to protonation and stabilize any carbocation formed post dehydration by the inductive and mesomeric effects of the *para*-hydroxy group. Through isolating the effects of each functional group, the role of functionality on the cleavage of the β-*O*-4 ether linkage can be identified and used to establish the mechanism.

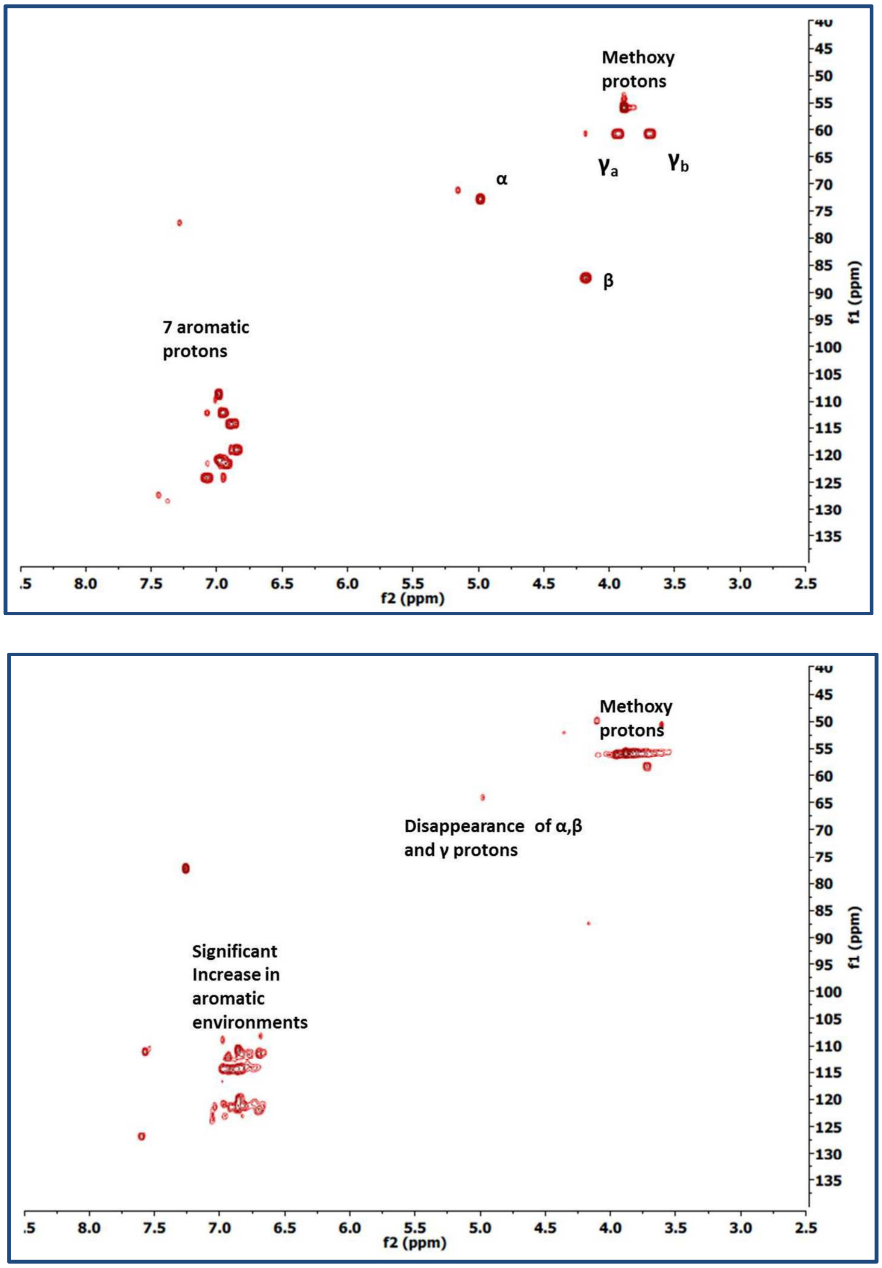

**Fig 7.** HSQC data of (a) commercial compound **I** (above) and (b) after reaction in $[C_4C_1im][HSO_4]_{10\%\ acid}$ and 20 (wt/wt) % water after 5 hours of reaction at 100 °C (below)

The modification of functionality on each of the model compounds allows one to assess the effects of the presence of common functionalities around the ether as well as around the aromatic ring attached to the α carbon, with results summarized in Table 1. The electron donating capabilities of the substituents on the aryl group adjacent to the α carbon have been quantified by combining the Hammett σ values of these substituents.[28] These values have been included in Table 1. Qualitative analysis of the HSQC spectra provided identification of the presence of the protons located on the α and β carbons (visible at 4.99, 72.22 ppm and 4.18, 72.77 ppm) representative of the β-*O*-4 ether linkage. Compound **I** was shown to completely cleave as expected, with all protons on the α and β carbons absent in the spectra (Fig. 7). When all functionality was removed apart from the ability to dehydrate, as in compound **II**, the β-*O*-4 ether linkage remained intact. The addition of an electron donating methoxy group *ortho* to the ring adjacent to the ether, as in compound **III,** also failed to lead to ether cleavage. However, on incorporating two further methoxy groups on the aromatic ring adjacent to the α carbon, full cleavage of the ether was observed as is the case with compound **IV**. Similarly compound **V,** bearing the same functionality as **I** with the sole difference being a benzylether group in place of the *para* hydroxy group was also shown to cleave. The increased intensity in the signal of the methoxy groups in 3.5 – 4 ppm region as well as the disappearance of the α and β protons signify hydrolysis of the β-*O*-4 linkage and the formation of the guaiacol product. The ability of compounds **IV** and **V** to completely hydrolyze suggests the electron donating methoxy groups on the aromatic ring adjacent to the site of dehydration are required to stabilize the carbocation produced on the loss of water. This trend follows the trend of σ values, with the ability of the substituents to stabilize the carbocation following the order: **I** > **V** > **IV** >> **II=III**.

**Table 1:** Ether cleavage of Model Compounds (**I-V**) in $[C_4C_1im][HSO_4]_{10\%\ acid}$

| **Compound** | **Functionality on Aromatic adjacent to α hydroxy** | **σ values of substituents on Aromatic adjacent to α hydroxy** | **Functionality on Aromatic adjacent to ether** | **α signal of substrate ($^1$H, $^{13}$C in ppm)** | **β signal of substrate ($^1$H, $^{13}$C in ppm)** | **α signal after reaction ($^1$H, $^{13}$C in ppm)** | **β signal after reaction ($^1$H, $^{13}$C in ppm)** | **β-*O*-4 linkage** |
|---|---|---|---|---|---|---|---|---|
| **I** | *p*-OH, *m*-OMe | -0.255 | *o*-OMe | 4.99, 72.77 | 4.18, 87.32 | n/a | n/a | Full cleavage occurs |
| **II** | n/a | 0 | n/a | 5.16, 72.64 | 4.14, 73.33 and 4.05, 73.34 | 5.16, 72.64 | 4.13, 73.34 and 4.06, 73.32 | No cleavage occurs |
| **III** | n/a | 0 | *o*-OMe | 5.14, 72.34 | 4.21, 76.38 and 4.01, 76.35 | 5.12, 72.33 | 4.18, 76.33 and 3.99, 76.31 | No cleavage occurs |
| **IV** | *p*-OMe, *m*-OMe | -0.153 | *o*-OMe | 5.07, 72.21 | 4.18, 76.51 and 3.99, 76.42 | Not visible | Not visible | Full cleavage occurs |
| **V** | *p*-OBn, *m*-OMe | -0.205 | *o*-OMe | 4.15, 87.34. | 4.97, 72.72 | Not visible | Not visible | Full cleavage occurs |

The high solubility of compounds **I** and **V** compared to the other model compounds gives some insight into the mechanism behind the increased solubility of lignin in acidic ILs. Interaction of the IL with the γ-hydroxymethyl group in these compounds was observed leading to the appearance of a new set of diastereotopic γ-protons before cleavage, as well as a new set of β and α signals (Fig 8). This suggests the $[HSO_4]^-$ anion has the ability to either strongly hydrogen bond with the γ-hydroxymethyl group or to react directly to form a sulfate group. The ability of the anion to interact strongly with this hydroxyl group has been implicated in preventing the loss of the γ-hydroxymethyl group as formaldehyde.[2,20] However, the HSQC spectra show the loss of the γ-methylene group as the cleaved products are formed in the presence of sulfuric acid, illustrating that deformylation occurs despite the strong interaction with the IL anion, consistent with previous observations for isolated lignin.[18] GC-MS analysis of all the model compounds confirmed that only compounds **I, IV** and **V** had the cleaved product guaiacol in the reaction mixture, whilst reaction mixtures with compounds **II** and **III** showing only the starting material. These substituent effects are consistent with those found by Sturgeon *et al.* for the cleavage of structurally related model compounds in acidic aqueous systems.[24] These studies all confirm the importance of dehydration prior to ether hydrolysis where an unstable intermediate is formed that immediately leads to cleavage.

The HSQC spectra also illustrate that no condensation products arising from the reaction of guaiacol could be observed due to the absence of signals in the aliphatic region of the spectra. These condensation reactions have been identified as the major pathway for the further reaction of guaiacol, affirming that the hydrolysis to guaiacol is the dominant pathway for ether cleavage. The loss of formaldehyde or sulfation of the γ-hydroxymethyl group would not affect the formation of guaiacol following ether cleavage, justifying its selection as a representative compound for understanding the kinetics of the ether hydrolysis reaction.

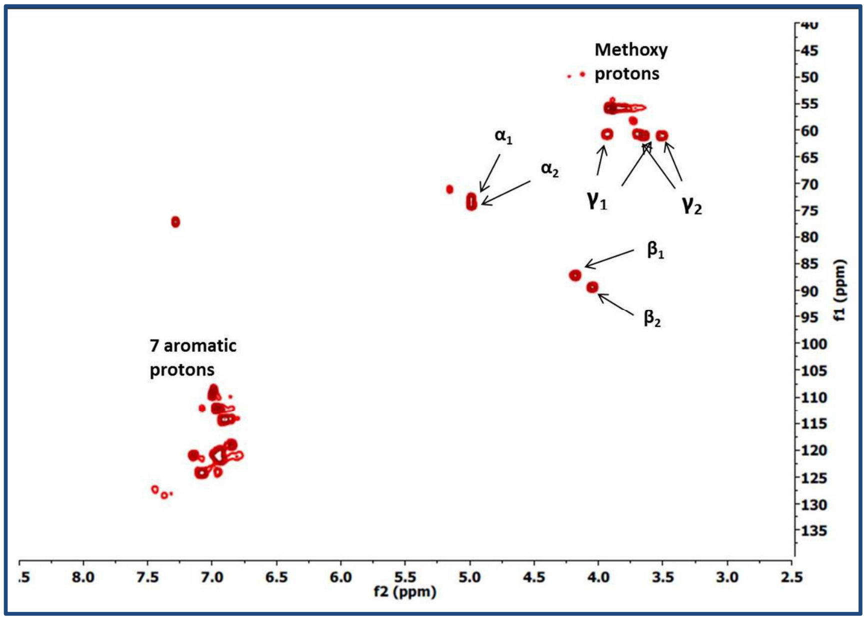

**Fig. 8** HSQC of compound **I** after 1 hour reaction in $[C_4C_1im][HSO_4]$ with 16.67 (wt/wt) % water:IL.

## Establishing a kinetic model

The key findings from Cox[19,20] and Binder[29] on the reactivity of compound **I** in a range of Brønsted acidic and Lewis acidic ILs show the importance of acidity in catalyzing ether cleavage in lignin. It has been repeatedly postulated in ionic systems that ether cleavage occurs as a consequence of a dehydration reaction after protonation of the hydroxy group located on the α carbon, yielding a stabilized carbocation.[18,19,22] This can then form an unsaturated enol-ether which can subsequently undergo acid hydrolysis to form guaiacol and the lesser understood "Hibbert ketone", as shown in Fig. 9. The overall rate expression depends on the rate determining step of the reaction. The two distinct steps in the cleavage of the linkage can be summarized as dehydration, involving protonation and loss of water, followed by hydrolysis, involving tautomerization of the enol-ether to a keto-ether and nucleophilic attack at the β carbon to liberate guaiacol.

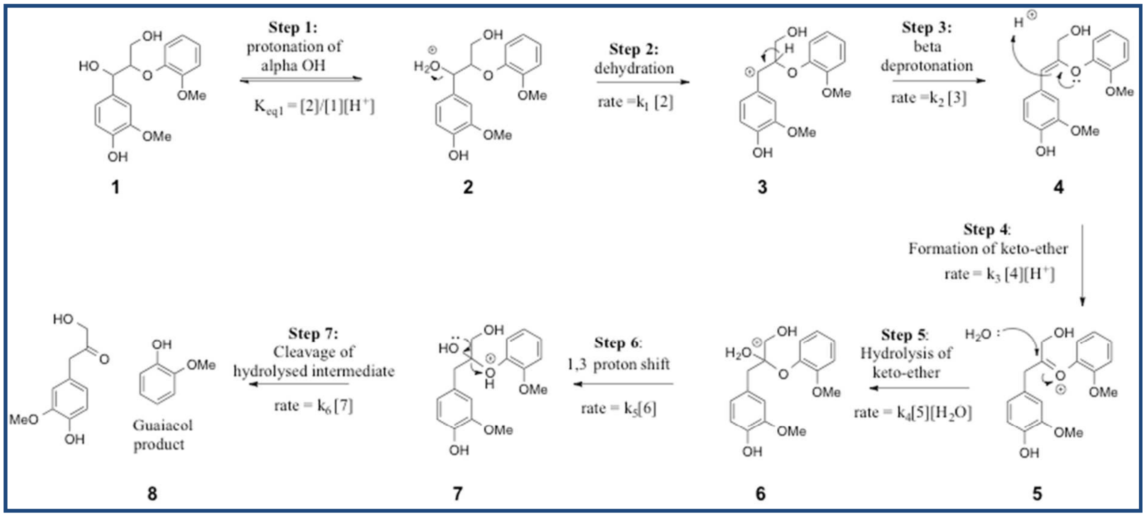

**Fig. 9** Acid catalyzed mechanism of compound **I** hydrolysis

The rate expression for the dehydration of compound **I** to intermediate **3**, involves the initial protonation of the hydroxyl group on the α-carbon of **1**, forming a concentration of intermediate denoted by the equilibrium constant $K_{eq1}$ which then undergoes dehydration:

$$d[\mathbf{3}]/dt = K_{eq1}\, k_1[\mathbf{1}][H^+]$$

The rate expression for the subsequent hydrolysis, involves the deprotonation of the β proton forming the dehydrated enol-ether substrate denoted as **4** (as shown after step 3) which then forms the keto-ether **5** which undergoes nucleophilic attack of water. This is then followed by a 1,3 proton shift to the basic ethereal oxygen to form an oxonium intermediate which readily cleaves to give the guaiacol product:

$$d[8]/dt = k_2k_3k_4\, k_5\, k_6\, [\mathbf{3}][H_2O][H^+]$$

The fundamental difference in both steps encompasses the opposite roles of water. For dehydration, the increased concentration of water would decrease the rate, whereas in hydrolysis, water is the active nucleophile therefore an increase in its concentration would increase rate.

From the kinetic data and the investigation of model compound functionality, it can be empirically concluded that lignin model compounds bearing the β-*O*-4 bond cleave following the initial rate expression, i.e. an initial protonation followed by dehydration. Therefore, in order to promote this initial step, electron donating groups are required to stabilize the newly formed carbocation.

**Eyring Activation Parameters for the dehydration of compound I**

The hydrolysis of compound **I** in [$C_4C_1$im][$HSO_4$] and other acidic ILs was studied to determine the effect of varying the IL cation. Aromatic and alkyl-ammonium ILs (**Fig. 2**) were prepared *via* alkylation for the aprotic set of ILs and direct acid-base neutralization for the protic set (see ESI). With a system of 16.67 (wt/wt) % water to ionic liquid, all the ILs employed gave faster cleavage of the substrate at 100 °C compared to [$C_4C_1$im][$HSO_4$] with yields reaching 36 % after a one-hour reaction time (**Fig. 10)**. Kinetic data for each IL fit well to a pseudo-first order model. The ammonium ionic liquids [$N_{4110}$][$HSO_4$] and [$N_{4111}$][$HSO_4$] provided the fastest hydrolysis of **I** with rate constants of 1.46 x $10^{-4}$ $s^{-1}$ and 9.20 x $10^{-5}$ $s^{-1}$ respectively (**Table 1**.).

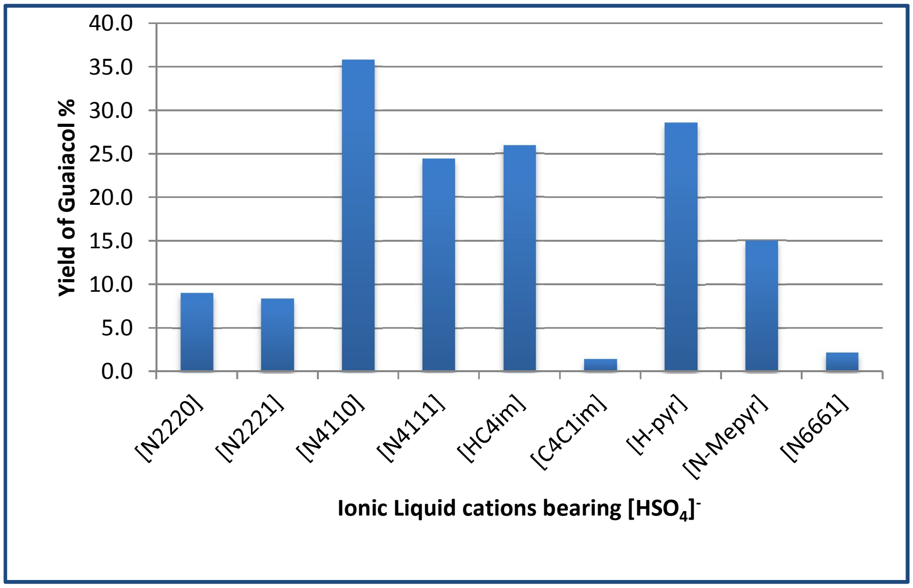

**Fig. 10**. Guaiacol yield from the hydrolysis of **I** with a range of [$HSO_4$]$^-$ ILs after a one hour reaction time at 100 °C

**Table 2.** Pseudo-first order rate constants for the hydrolysis of **I** with a range of $[HSO_4]^-$ ILs. Reactions carried out with 16.67 (wt/wt) % water:IL at 100 °C

| **Entry** | **Ionic Liquid** | **Ionic liquid type** | **Rate Constant ($s^{-1} \times 10^{-6}$)** |
|---|---|---|---|
| 1 | $[C_4C_1im][HSO_4]$ | Aprotic, imidazolium | 5.24 |
| 2 | $[HC_4im][HSO_4]$ | Protic, imidazolim | 64.6 |
| 3 | [*N*-MePyr]$[HSO_4]$ | Aprotic, aromatic | 54.8 |
| 4 | $[HPyr][HSO_4]$ | Protic, aromatic | 50.1 |
| 5 | $[N_{4111}][HSO_4]$ | Aprotic, ammonium | 92.0 |
| 6 | $[N_{4110}][HSO_4]$ | Protic, ammonium | 146 |
| 7 | $[N_{2221}][HSO_4]$ | Aprotic, ammonium | 23.7 |
| 8 | $[N_{2220}][HSO_4]$ | Protic, ammonium | 11.7 |
| 9 | $[N_{6661}][HSO_4]$ | Aprotic, ammonium | 18.8 |

The kinetic data reported in Table 2 show no noticeable trend regarding choice of cation, apart from the reaction in $[C_4C_1im][HSO_4]$ being significantly slower compared to the other ILs. Furthermore, ILs containing $[N_{411x}]$ cations show a substantial increase in rate by around half an order of magnitude compared to all the other ILs. In order to gain more insight into the microscopic role of solvent-solute interactions with acidic ILs, kinetic data from multiple temperatures between 90-120 °C were obtained and Eyring plots generated for each IL. From these plots $\Delta H^{\ddagger}$ and $\Delta S^{\ddagger}$ can be obtained and consequently the Gibbs free energy of activation. As the rate-determining step is dehydration, the $[HSO_4]^-$ anion is envisaged to stabilize the starting material or activated complex during dissociation of water from the protonated intermediate. According to the Hughes-Ingold rules,[30] an increase in the dispersal of charge on progression from the initial state to the activated complex would decrease the relative effect of solvation on the activated complex. This therefore leads to preferential solvation of the initial molecule whereby charge density in the activated complex is lower than that of the initial substrate. As the substrate has the cationic character concentrated on the α-hydroxy moiety, organization of the anion around the positively charged solute occurs. This would imply an increase in reaction rate when an IL with higher cation-anion association is employed as shown in **Table 2** and depicted schematically in **Fig. 11**.

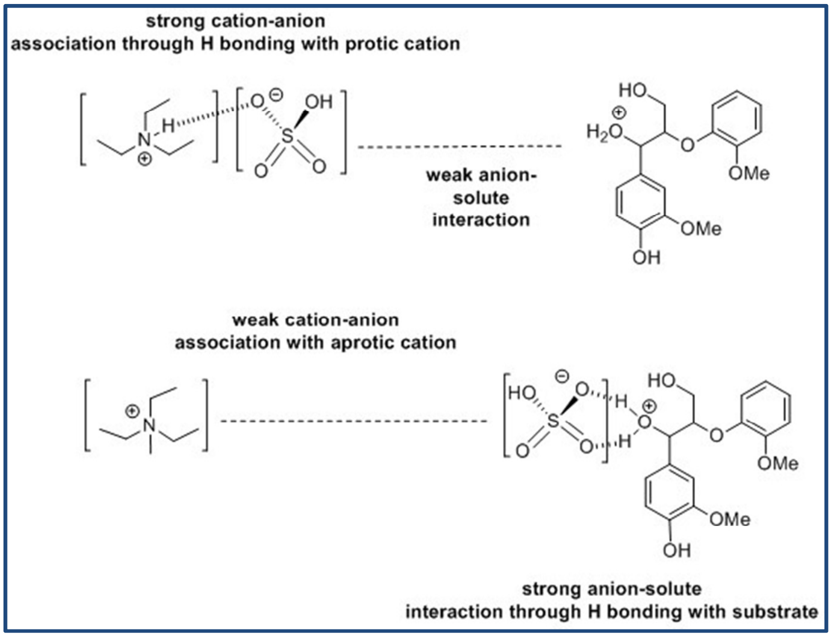

**Fig. 11.** Schematic illustrating the effect of cation-anion interactions within $[N_{222x}][HSO_4]$ ILs on the solvation of the oxonium intermediate prior to the dissociation of water to form the activated complex.

As expected, the reactions with the fastest rates have the lowest $\Delta G^‡$ values. $[C_4C_1im][HSO_4]$ has the highest Gibbs free energy of activation with the other ILs displaying similar values as shown in Table 2. The effects of enthalpy are shown to dominate $\Delta G^‡$ and all protic ILs (apart from those containing butylimidazolium cations) exhibit lower enthalpies of activation compared to their aprotic counterpart. This is compensated by a decreased $\Delta S^‡$ in each case. Our interpretation of these values of $\Delta H^‡$ can be rationalized by the stronger cation-anion association due to stronger hydrogen bonding between the protic ammonium cation and the anion. With stronger cation-anion association, the anion weakens its interaction with the cationic oxonium intermediate leading to a significant decrease in the value of $\Delta H^‡$. This can be conceptualized by considering the initial oxonium intermediate; weaker interactions between the solvent and this intermediate would increase its initial energy, subsequently showing a lower difference in enthalpy of activation between the starting material and the activated complex. This trend can be observed further with the trend in ammonium cations. Asymmetric cations bearing one single long alkyl chain, such as $[N_{4110}][HSO_4]$ and $[N_{4111}][HSO_4]$, have stronger cation-anion association and give lower values of $\Delta H^‡$. This can be compared to their isomers with greater steric bulk around the nitrogen center: $[N_{2221}][HSO_4]$ and $[N_{2220}][HSO_4]$, whereby the presence of three ethyl chains on the cation increases the steric shielding between the cation and anion which reduces the strength of their association. This therefore allows the anion to interact more strongly with the solute, leading to an increase in the value of $\Delta H^‡$ by 33.9 kJ mol$^{-1}$ for the protic set and 4.1 kJ mol$^{-1}$ for the aprotic set relative to the $[N_{411x}][HSO_4]$ ILs. The heavily hindered cation $[N_{6661}][HSO_4]$ further supports this rationale, as the large size of the three hexyl groups around the cationic center as well as the lack of hydrogen bonding further reduces associative forces between ions, increasing the ability of the anion to solvate the solute, leading to the highest enthalpy of activation at 131.8 kJ mol$^{-1}$. In terms of the absolute values of $\Delta H^‡$, the high enthalpy of activation indicates a unimolecular E1 mechanism in which the protonated substrate dehydrates with the loss of water being rate limiting. The alternative E2 mechanism would proceed directly through an enol-ether with the concerted abstraction of the β proton and water. Such a pathway would have a significantly lower enthalpy of activation than was observed here. This is supported by similar examples of unimolecular reactions in ILs for which high values of $\Delta H^{\ddagger}$ have been reported.[31] The $\Delta S^{\ddagger}$ values further support this. E1 processes typically exhibit small $\Delta S^{\ddagger}$ values around 0 J $K^{-1}$ $mol^{-1}$ due to the increased disorder of the activated complex, with these values becoming more negative due to the electrostriction of the solvent around the substrate. For an E2 process, the $\Delta S^{\ddagger}$ values would be much more negative than those observed here**.**

**Table 3.** Eyring Activation Parameters for the dehydration of **I** in a range of $[HSO_4]^-$ ILs taken between 90 °C and 120 °C. Uncertainties are derived from the standard errors of the parameters extracted from the linear fits obtained from the Eyring plots (see ESI)

| **Entry** | **Ionic Liquid** | $\Delta H^{\ddagger}$ **(kJ mol$^{-1}$)** | $\Delta S^{\ddagger}$ **(JK$^{-1}$ mol$^{-1}$)** | $T\Delta S_{373K}^{\ddagger}$ **(kJ mol$^{-1}$)** | $\Delta G_{373K}^{\ddagger}$ **(kJ mol$^{-1}$)** |
|---|---|---|---|---|---|
| 1 | $[C_4C_1im][HSO_4]$ | 104 ± 6 | -70 ± 19 | -26 ± 7 | 130 ± 9 |
| 2 | $[HC_4im][HSO_4]$ | 118 ± 6 | -10 ± 15 | -4 ± 6 | 122 ± 8 |
| 3 | $[HPyr][HSO_4]$ | 84 ± 11 | -99 ± 30 | -37 ± 11 | 121 ± 16 |
| 4 | [*N*-MePyr]$[HSO_4]$ | 103 ± 6 | -52 ± 16 | -13 ± 6 | 122 ± 8 |
| 5 | $[N_{4111}][HSO_4]$ | 121 ± 9 | 0 ± 23 | 0 ± 9 | 121 ± 12 |
| 6 | $[N_{4110}][HSO_4]$ | 75 ± 11 | -121 ± 28 | -45 ± 10 | 120 ± 15 |
| 7 | $[N_{2220}][HSO_4]$ | 109 ± 2 | -50 ± 6 | -19 ± 2 | 127 ± 3 |
| 8 | $[N_{2221}][HSO_4]$ | 126 ± 13 | 4 ± 34 | 0 ± 13 | 125 ± 18 |
| 9 | $[N_{6661}][HSO_4]$ | 132 ± 11 | 16 ± 28 | 6 ± 11 | 126 ± 15 |

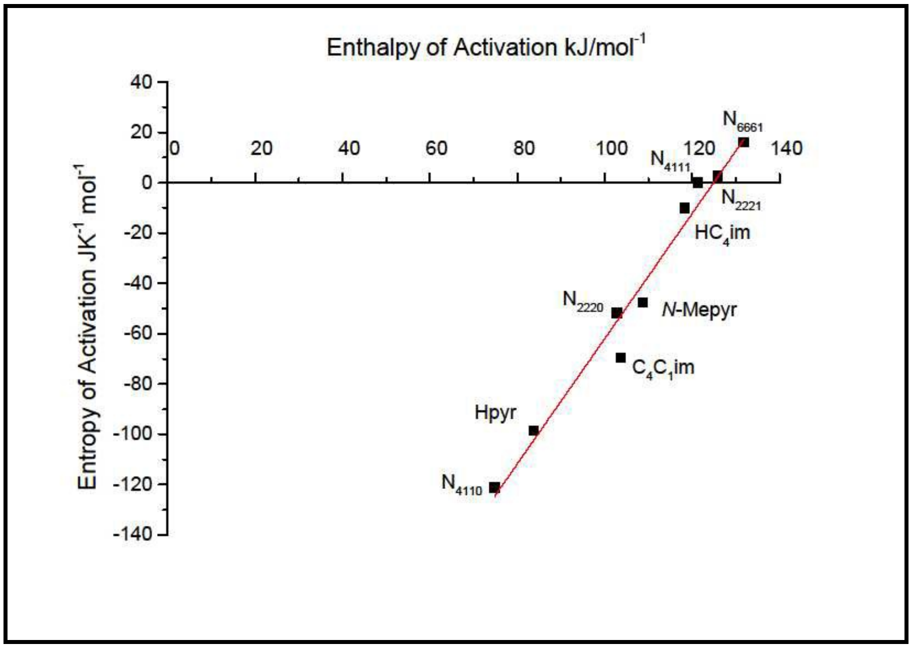

**Fig. 12.** Isokinetic plot showing enthalpy-entropy compensation of the dehydration of compound **I** in a range of $[HSO_4]^-$ ILs.

Through plotting $\Delta S^\ddagger$ against $\Delta H^\ddagger$, an almost complete compensation between entropy and enthalpy of activation is observed with each IL, indicating the same mechanism holds in all cases, an effect that has been reported previously.[32,33] The results are consistent with the dehydration mechanism postulated. The trends observed with each IL conclude the importance of cation-anion association in determining the enthalpy of activation and implies that choosing ILs with a high degree of cation-anion association, preferably *via* the introduction of hydrogen bonding, could increase the rate of ether cleavage at lower temperatures.

## Discussion

The results obtained here illustrate that the hydrolysis of model compounds bearing β-*O*-4 linkages within ILs containing the $[HSO_4]^-$ anion proceed through a similar mechanism to those within aqueous acidic systems.[24,34] Specifically, the mechanism proceeds by the protonation of the α-hydroxyl group and loss of water with the latter step being rate determining. Consequently, the dehydration and resultant ether cleavage proceed faster in the presence of electron donating substituents due to the mesomeric stabilisation of the carbocation formed. A similar mechanism has also been predicted by Janesko where DFT calculations were used to show that the dehydration of compound II proceeded *via* an E1 mechanism, with the stability of the carbocation essential for reaction,[26]The HSQC results here illustrate that significant deformylation occurs despite evidence of a strong interaction with $[HSO_4]^-$. The strong interaction of anions with the γ-hydroxymethyl group has been implicated in the prevention of the loss of formaldehyde,[20,34] however it appears that the interaction with $[HSO_4]^-$ is unable to prevent this, despite being sufficiently strong as to lead to additional γ-methyl $^1H$ signals. This is consistent with results in aqueous or aqueous/organic systems where sulfuric acid was found to lead to deformylation whereas acids with more coordinating anions such as HCl or HBr yielded fewer deformylated products.

Given the quantitative kinetic data obtained from this study, an examination of how the rate of ether cleavage compares with other solvent environments was carried out. While temperature effects can be approximated by extrapolation from the variable temperature results using the Eyring equation, the lack of a straightforward correlation between rates and acid concentrations complicates the comparison of reaction rates between systems. Nonetheless, the standard aqueous or aqueous/organic reaction conditions generally feature sulfuric acid concentrations of the order of 0.1 M which would have $H_0 < 1$ due to the convergence of pH and Hammett acidity scales in dilute aqueous solutions and the weaker dissociation of the second proton. Hence the IL systems used here, with $H_0 > 2$ are likely to be less acidic than the reactions in aqueous environments and the resultant rates should be considered in this context.

With the foregoing in mind, Sturgeon *et al.* found the acidolysis of **I** to proceed with a pseudo-first order rate constant of $4.2 \times 10^{-4}$ $s^{-1}$ at 150 °C in 0.2 M aqueous $H_2SO_4$.[24] Notably this is the rate of the disappearance of **I** rather than guaiacol appearance, hence will overestimate the actual rate of ether cleavage. The largest extrapolated rate of cleavage occurs within $[N_{4111}][HSO_4]$ at 150 °C, with an extrapolated rate constant of $1.02 \times 10^{-2}$ $s^{-1}$. That is, the rate of ether cleavage would be 25 times faster in this IL despite the much lower acidity of the reaction conditions employed compared to the aqueous system. Even the worst performing IL

([$C_4C_1$im][$HSO_4$]) would yield a rate constant of 2.8 × $10^{-4}$ $s^{-1}$, of the same order as the aqueous reaction despite the much lower acidity.

The acidolysis of a compound closely related to **I** the only difference being a p-OMe rather than p-OH group, has been studied by Imai *et al.*[35] These reactions were performed at 85 °C in an 82:18 1,4-dioxane:water mixture with 0.1 M $H_2SO_4$. The rate of cleavage for this ether was found to be 2.2 × $10^{-6}$ $s^{-1}$. Extrapolating to this temperature, the IL which would provide the fastest rates under these conditions would be [$N_{4110}$][$HSO_4$], with a rate constant of 4.1 × $10^{-5}$ $s^{-1}$, nearly 20 times faster than the aqueous/organic solvent system. Even [$C_4C_1$im][$HSO_4$], the IL predicted to give the slowest rate, would be comparable with this solvent system with a rate of 1.1 × $10^{-6}$ $s^{-1}$ despite its lower acidity and the aforementioned discrepancy in measurement which would lead to an overestimate of the specific rate of ether cleavage for Imai *et al*. Tabulated data of the extrapolated rate constants under both these conditions and those of Sturgeon *et al.* are provided in the ESI. From comparing the rates within these ILs with aqueous or aqueous/organic solvents it is evident that ILs based on the [$HSO_4$]$^-$ anion are effective media for facilitating the cleavage of β-*O*-4 ether linkages even in the absence of added acid. The different ILs expected to provide the fastest and slowest rate at each temperature highlights the importance of understanding solvent-solute interactions to enable rational IL selection and design. This reinforces that ether cleavage can be promoted at lower temperatures by this class of ILs through the selection of a cation which is able to strongly interact with the [$HSO_4$]$^-$ anion.

## Conclusions

It was found that the mechanism of lignin's β-*O*-4 linkage hydrolysis in all of the [$HSO_4$]$^-$ ILs proceeded *via* an acid catalysed reaction whereby the rate determining step involves initial protonation followed by dehydration. This conclusion was supported using kinetic tools where water and acid concentration were varied and the functionality of the reaction substrate was modified. Through the use of an Eyring plot, insight into the effects of cation choice was also gained. The Gibbs energy of activation remained approximately consistent in each IL system with an average of 124 kJ $mol^{-1}$. The observed high enthalpies of activation indicated that dehydration occurs *via* an E1 mechanism and the differences in these values were almost fully compensated by the entropic component. These differences are attributed to the associative forces between the cation and anion, influenced primarily by hydrogen bonding, determining the degree of solvation of the protonated solute. We conclude that whilst the [$HSO_4$]$^-$ anion is effective at cleaving the β-*O*-4 ether linkage, anion-cation association plays a significant role in determining solvation of the solute and therefore the rate of reaction. This therefore provides scope for the appropriate design of IL cations for successful lignin depolymerisation and processing at lower temperatures, with these results suggesting that this would be favoured by ILs with increased cation-anion association.

### Acknowledgements

The authors wish to thank the UK Engineering and Physical Sciences Research Council (EP/K014676/1) for support.

### References

(1) Boerjan, W.; Ralph, J.; Baucher, M. *Ann. Rev. Plant. Biol.* **2003**, *54*, 519.

(2) Brandt, A.; Gräsvik, J.; Hallett, J. P.; Welton, T. *Green Chem.* **2013**, *15* (3), 550.

(3) El Hage, R.; Brosse, N.; Chrusciel, L.; Sanchez, C.; Sannigrahi, P.; Ragauskas, A. *Polym. Degrad. Stabil.* **2009**, *94* (10), 1632.

(4) Miyafuji, H. *Wood. Sci*. **2015**, *61*, 343-350

(5) Mäki-Arvela, P.; Anugwom, I.; Virtanen, P.; Sjöholm, R.; Mikkola, J. P. *Ind. Crop. Prod.* **2010**, *32* (3), 175.

(6) Fort, D. A.; Remsing, R. C.; Swatloski, R. P.; Moyna, P.; Rogers, R. D. *Green Chem.* **2007**, *9*, 63.

(7) Kilpeläinen, I.; Xie, H.; King, A.; Granstrom, M.; Heikkinen, S.; Argyropoulos, D. *J. Agric. Food Chem.* **2007**, *55*, 9142.

(8) Swatloski, R. P.; Spear, S. K.; Holbrey, J. D.; Rogers, R. D. *J. Am. Chem. Soc.* **2002**, *124* (18), 4974.

(9) Pinkert, A.; Marsh, K. N.; Pang, S.; Staiger, M. . *Chem. Rev.* **2009**, *109*, 6712.

(10) Pu, Y.; Jiang, N.; Ragauskas, A. J. *J. Wood. Chem. Technol.* **2007**, *27* (1), 23.

(11) Brandt, A.; Ray, M. J.; To, T. Q.; Leak, D. J.; Murphy, R. J.; Welton, T. *Green Chem.* **2011**, *13* (9), 2489.

(12) Kline, L. M.; Hayes, D. G.; Womac, A. R.; Labbé, N. *Bioresources* **2010**, *5* (3), 1366.

(13) Prado, R.; Erdocia, X.; Labidi, J. *J. Chem. Technol. Biol.* **2013**, *88* (7), 1248.

(14) Hallett, J. P.; Welton, T. *Chem. Rev.* **2011**, *111* (5), 3508.

(15) Verdía, P.; Brandt, A.; Hallett, J. P.; Ray, M. J.; Welton, T. *Green Chem.* **2014**, *16* (3), 1617.

(16) George, A.; Tran, K.; Morgan, T. J.; Benke, P. I.; Berrueco, C.; Lorente, E.; Wu, B. C.; Keasling, J. D.; Simmons, B. a.; Holmes, B. M. *Green Chem.* **2011**, *13* (12), 3375./

(17) Wen, J.-L.; Yuan, T.-Q.; Sun, S.-L.; Xu, F.; Sun, R.-C. *Green Chem.* **2014**, 181.

(18) Brandt, A; Chen, L; Van Dongen, B. E; Welton, T; Hallett.; *Green Chem.* **2015**, *17*, 5019-5034(19)
Jia, S.; Cox, B. J.; Guo, X.; Zhang, Z. C.; Ekerdt, J. G. *ChemSusChem* **2010**, *3* (9), 1078.

(20) Cox, B. J.; Jia, S.; Zhang, Z. C.; Ekerdt, J. G. *Polym. Degrad. Stabil.* **2011**, *96* (4), 426.

(21) Jia, S.; Cox, B. J.; Guo, X.; Zhang, Z. C.; Ekerdt, J. G. *Ind. Eng. Chem. Res* **2011**, *50*, 849.

(22) Kubo, S.; Hashida, K.; Yamada, T. *J. Wood Chem. Technol.* **2008**, *28*, 84.

(23) Cox, B. J.; Ekerdt, J. G. *Bioresour. Technol.* **2012**, *118*, 584.

(24) Sturgeon, M. R.; Kim, S.; Lawrence, K.; Paton, R. S.; Chmely, S. C.; Nimlos, M.; Foust, T. D.; Beckham, G. T. *ACS Sustain. Chem. Eng.* **2013**, *2* (3), 472.

(25) Gräsvik, J.; Hallett, J. P.; To, T. Q.; Welton, T. *Chem. Commun.* **2014**, *50*, 7258.

(26) Janesko, B.; *Phys Chem. Chem. Phys.* **2014**, *16*, 5423-5433

(27) McDaniel, D. H.; Brown, H.C; *J. Org. Chem.* **1958,** *23*, 420-427

(28) Yu, H.; Hu. J; Chang, J; *Ind. Eng. Chem. Res.* **2012**, *51*, 3452-3457

(29) Binder, J. B.; Gray, M. J.; White, J. F.; Zhang, Z. C.; Holladay, J. E. *Biomass and Bioenergy* **2009**, *33* (9), 1122.

(30) Reichardt, C. *Solvents and solvent effects in organic chemistry*; 2003.

(31) Yau, H. M.; Barnes, S. A; Hook, J. M.; Youngs, T. G. A; Croft, A. K.; Harper, J. B. *Chem. Commun.* **2008**, No. 30, 3576.

(32) Leffler, J. A. *J. Org. Chem.* **1955**, *20* (9), 1202.

(33) Jasinki, R. *Nature* **1964**, *201*, 489.

(34) Yokoyama, T. *J. Wood Chem. Technol.* **2014**, *35*, 27-41

(35) Imai, T.; Yokoyama, T.; *J. Wood. Sci.* **2011**, *57*, 219-225